

1 **Continuous monitoring of radon gas as a tool to understand air dynamics in the cave of**
2 **Altamira (Cantabria, Spain)**

3 Carlos Sainz^{a,b}, Daniel Rábago^a, Santiago Celaya^a, Enrique Fernández^a, Jorge Quindós^a, Luis
4 Quindós^a, Alicia Fernández^a, Ismael Fuente^a, Jose Luis Arteché^c, Luis Santiago Quindós^{a,b}

5 ^a Radon Group. University of Cantabria. C/Cardenal Herrera Oria s/n 39011, Santander, Spain

6 ^b The Cantabrian International Institute for Prehistoric Research (IIIPC)

7 ^c Spanish Meteorological Agency, AEMET

8 © 2018. This manuscript version is made available under the CC-BY-NC-ND 4.0 license <http://creativecommons.org/licenses/by-nc-nd/4.0/>

9 **Corresponding Author:** Daniel Rábago (daniel.rabago@unican.es)

10 **ABSTRACT**

11 **The use of radon as an atmospheric tracer in the Altamira Cave over the past 30 years has provided**
12 **relevant information about gaseous exchanges between the Polychromes Room, the adjoining**
13 **Chambers inside the cave, and the outside atmosphere. The relatively simple physico-chemical**
14 **behaviour of radon gas provides a marked advantage over other tracer gases that are usually present**
15 **in high concentrations in hypogeous environments, such as CO₂. Two types of continuous radon**
16 **measurement were undertaken. The first involves active detectors located in the Hall and Polychromes**
17 **Room, which provide radon concentration values at 1-hour intervals. In addition, nuclear solid track**
18 **etched detectors (CR-39) are used in every chamber of the cave over 14-day exposure periods, providing**
19 **average radon concentrations. In this paper we show some of the specific degassing and recharge**
20 **events identified by anomalous variations in the concentration of radon gas in the Polychromes Room.**
21 **In addition, we update knowledge regarding the degree of connection between chambers inside the**
22 **cave and with the outside atmosphere. We verify that the connection between the Polychromes Room**
23 **and the rest of the cave has been drastically reduced by the installation of the second closure in 2008.**
24 **Except for point exchanges with the Crossing zone generated by a negative temperature gradient in**
25 **that direction, the atmosphere of the Polychromes Room remains stable, or else it exchanges matter**
26 **with the outside atmosphere through the karst interface. The role of radon as a tracer is demonstrated**

27 to be valid both to reflect seasonal cycles of degassing and recharge, and to analyse shorter (daily)
28 period fluctuations.

29

30 **Keywords: Radon; Cave; Conservation; Carbon dioxide; Ventilation**

31 **1. INTRODUCTION**

32 The Cave of Altamira is known worldwide for the ancient rock art that it contains. The pictorial
33 representations dating back about 15,000 years, mainly concentrated in the so-called
34 Polychromes Room, are rank among the best artistic manifestations in the history of Humanity,
35 their value being not only symbolic, but also technical and representative (Lasheras et al., 2014).
36 Altamira Cave was named a World Heritage Site in 1985 by UNESCO
37 (<http://whc.unesco.org/en/list/310>).

38 Since its discovery in around 1868, the cave has been visited by a large number of people
39 attracted by the beauty and realism of the pictorial representations it contains. In 1977, the
40 great influx of visitors led to the decision to close the cave in order to conserve its cultural
41 heritage due to increase in CO₂, temperature and lighting which promote the development of
42 Lampenflora (Pfundler et al., 2018). During this first closure, scientific studies began to
43 investigate how best to conserve the paintings. These studies included a detailed analysis of
44 both the geological and environmental setting of the paintings, and the impact that the presence
45 of visitors exerted on their state of conservation (Villar et al., 1984b; 1986b). These studies
46 provided the first integral view of the physico-chemical conditions under which the paintings
47 were preserved, and provided the first models to explain the dynamics of gaseous exchanges
48 between the various chambers inside the cave and between the cave and the outside
49 environment (Villar et al., 1983; 1984a; 1985; 1986a). Thanks to the systematic acquisition of
50 further environmental data, and to the improvement of the theoretical models over successive
51 research projects, we currently have quite a complete and complex vision of the main thermal,

52 hydric and atmospheric processes that affect the conservation of the paintings, and also of the
53 possible impacts that the ingress of visitors would have on those processes (Soler et al., 1999;
54 Sánchez-Moral et al., 1999; 2010).

55 All work to date has used the concentration of radon gas (^{222}Rn) inside the cave to investigate
56 the atmospheric dynamics of the Altamira Cave, (Fernández et al., 1986; Lario et al., 2005;
57 Cuezva et al., 2011; Garcia-Anton et al., 2014). It is well known that radon is a natural radioactive
58 gas that comes from the disintegration of the ^{226}Ra present in variable amounts in most rocks
59 and soils of the earth's crust; radon tends to accumulate in poorly ventilated ground or
60 underground enclosures (Quindós et al., 1991). Radon gas has been used as a tracer of dynamic
61 processes in aqueous and aerial media on numerous occasions (Fernández et al., 1984; Frisia et
62 al., 2011; Kowalczk and Froelich, 2010; Sainz et al., 2016). The relatively simple physico-chemical
63 behaviour of radon gas means that it has a marked advantage over other tracer gases, such as
64 CO_2 , which are usually present in high concentrations in hypogeous environments (Batiot-Guilhe
65 et al., 2007; Nazaroff and Nero, 1988). The generation of radon gas inside the cave can be
66 considered practically constant as there are no processes that significantly alter either the
67 concentration of ^{226}Ra in the rock or the emission of radon over its surfaces. For this reason,
68 positive increments in radon concentration inside a rock chamber can only be due to its
69 increased isolation with respect to the outside atmosphere, which typically has very low radon
70 concentrations, or to a supply of air from adjacent chambers containing significantly higher
71 concentrations of the gas. Likewise, reductions in radon concentration in such a chamber can
72 only be produced by radioactive decay or due to an air supply containing a lower concentration
73 of the gas, usually from more superficial or external locations. Radon is a noble gas, which makes
74 it highly unlikely that its concentration reduces by means of chemical reactions with the
75 environment in which it is found (Nazaroff and Nero, 1988).

76 Over the past 30 years, the use of radon as an atmospheric tracer in Altamira Cave has provided
77 relevant information about gaseous exchange between the Polychromes Room, the adjoining
78 chambers inside the cave, and the exterior atmosphere. During the 1980s the first estimates of
79 the rates of air exchange between the Polychromes Room and the large hall inside the cave
80 entrance, called the Hall, were made (Fernández et al., 1986). By also using the CO₂
81 concentrations, they proposed a model of air exchange which was driven by the temperature
82 gradient between the two chambers at different times of the year. In 2008, this connection was
83 significantly altered with the installation of a second seal door designed to reduce the ingress of
84 organic matter into the Polychromes Room and to stabilise its temperature. Later studies
85 provided detailed descriptions of the exchange processes between the Polychromes Room and
86 the exterior through the karst host rock (Sánchez-Moral et al., 2009; 2012; Somavilla et al.,
87 1978).

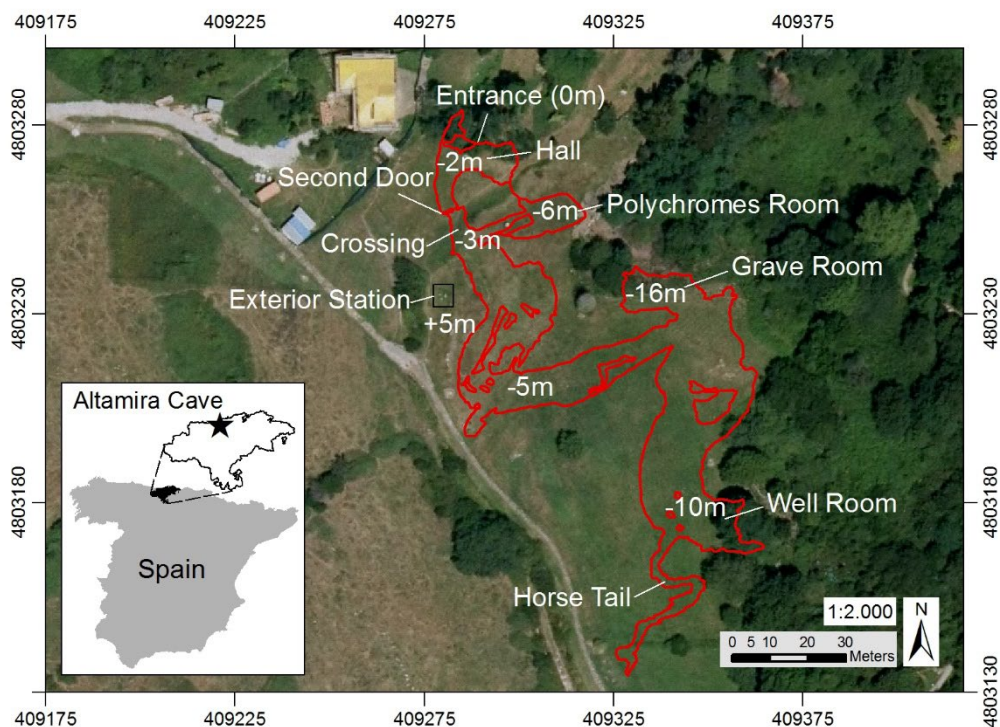
88 As in other caves, the seasonal loading and discharging of gases in the Altamira Cave –
89 particularly in the Polychromes Room – are easily visualised by continuous monitoring of radon
90 and CO₂ concentrations (Cuezva et al., 2011). In deep caves, with a single point of connection
91 with the outside, usually the entrance, concentrations of radon and CO₂ are at a maximum in
92 summer, and at a minimum in winter. These dynamics can be easily explained by the mass
93 displacements that are caused by differences in air density between the cave interior and
94 exterior at different times of year. However, the Cave of Altamira is quite shallow – the
95 overburden above its ceilings varies from 2 to 10 m, although it can reach 18 m in places (Elez
96 et al., 2013). Its karstic configuration favours gaseous exchange with the exterior through parts
97 of the cavity other than the main entrance. For this reason, the dynamics of tracer gas
98 concentrations (such as Rn and CO₂) can be very different, or even opposite to what is usually
99 observed in deep caves.

100 This overall dynamics of gas exchange within Altamira Cave has various exceptions, such as in
101 the event of an abrupt change or inversion of the temperature gradient between the outer and
102 inner atmosphere of the cave. This article outlines some specific degassing and recharge events
103 identified by anomalous variations in radon gas concentration in the Polychromes Room. In
104 addition, knowledge about the degree of connection between Chambers inside the cave and
105 between these and the outside atmosphere is updated.

106 2. MATERIAL AND METHODS

107 2.1 Location and characteristics of the Altamira Cave

108 The Altamira Cave is located in Santillana del Mar (Cantabria, Spain) at an elevation of more than
109 150 m above sea level. Its entrance faces North and the cave as a whole is oriented northwest.
110 It is a rather shallow cave, with a difference in elevation of around 16 m between the level of
111 the entrance and its deepest point of (Fig. 1).



112

113 Fig. 1. Plan of the Altamira Cave superposed on an orthophoto. The differences in height shown
114 are relative to the elevation at the cave entrance.

115 About 25 m from the entrance, just beyond the second artificial door, is a junction, called El
116 Cruce ('The Crossing'). Ahead lies the access to the deeper chambers of the cave, while to the
117 left, descending about 2 m via some stairs, is the access to the Polychromes Room. This chamber
118 is about 15 m long and 7 m wide, with an average height of less than 3 m; it is here that the
119 spectacular coloured pictorial representations on the ceiling were made, which led to the cave
120 being dubbed the 'Sistine Chapel' of Quaternary Art (Déchelette, 1908; Elez et al., 2013) The
121 volume of the Polychromes Room is approximately 342 m³ and the ceiling area is 159 m².

122 The microclimate inside the cave is characterised by very stable temperatures throughout the
123 year, with a thermal oscillation in the Polychromes Room of less than 2 °C. This oscillation is
124 described by a sinusoidal wave that is out of phase and damped with respect to the annual
125 thermal oscillation outside. This is due to the layer of rock between the ceiling of the chamber
126 and the ground surface immediately above.

127 **2.2 Radon gas concentration measurements**

128 Two types of continuous radon measurement are made inside the Cave of Altamira. The first
129 involves active detectors located in the Hall and Polychromes Room, which provide radon
130 concentration at 1-hour intervals. In addition, in every chamber of the cave, nuclear solid track
131 etched detectors (CR-39) provide averaged radon concentrations over exposure periods of two
132 weeks.

133 RadonScout monitors (SARAD GmbH) are used for the continuous radon measurements, their
134 sensors are Si detectors that converts the energy yielded by alpha emissions of radon and its
135 progeny into electrical impulses whose magnitude is proportional to the energy absorbed. This
136 device performs alpha spectrometry to measure the amount of radon in the air. Measurements
137 can be made at intervals of between 1 and 3 h, and are written to memory, allowing storage of
138 data series more than two months long. Concentrations can be measured in the range 0 to 10
139 MBq/m³. The uncertainty associated with the measurement performed by this device varies

140 from 20 % to 10 % in the concentration range of 100-1000 Bq/m³. Each RadonScout monitor is
141 calibrated every six months in LaRUC radon chamber described below, using an AlphaGUARD
142 (SAPHIMO GmbH) device as reference traceable to the PTB (*Physikalisch Technische*
143 *Bundesanstalt*) ²²²Rn chamber (Germany) of using a primary PTB gaseous ²²²Rn activity standard.
144 In addition, detection efficiency is verified in the data download performed every two weeks.

145 The main difficulty presented by the continuous measurement of the radon concentration in
146 underground environments is the continuously high relative humidity of the cave atmosphere.
147 In addition to possible damage to the electronic components of the monitors, high humidity can
148 modify detection efficiency in electrostatic radon descendant collection systems (George, 1996).
149 In order to minimise the influence of ambient humidity on the operation of continuous monitors,
150 they are placed in a low density waterproof plastic bag, which allows the transfer of radon
151 through its surface by diffusion. Following the procedure of Moreno et al. (2015), it has been
152 demonstrated in a controlled atmosphere that the radon measurement inside the bag implies
153 an initial delay in the response to changes in concentration between 3 and 6 hours. For this
154 reason, the first ten measurements are discarded.

155 In contrast, track etch detectors CR-39 (Radosys Ltd.) were used to obtain integrated values of
156 the radon concentration every 14 days. Measurements using these devices are based on the
157 effect of α particles on different plastic materials. Radon and its progeny emit α particles that
158 produce a track in the detector. The plastic material is placed in a container and radon diffuses
159 through the container preventing the entrance of its progeny. At the end of the measurement
160 period, the chamber is sealed and transferred to the laboratory, where it is analysed.

161 In the laboratory, the track etch detectors (consisting of a plastic polymer) are chemically
162 treated and the number of tracks per unit area of the detector is counted under a microscope
163 using an automatic optical reader. Microscope is checked, with a tolerance range, every time it
164 is used with a traceability slide where tracks density is known. Once the calibration factor of the

165 equipment is known, the number of tracks per unit area allows the radon concentration to be
166 calculated. The exposure time of these detectors varies depending on the range of
167 concentrations to be measured. The calibration factor is provided by the manufacturer, however
168 we do a double check using our radon chamber and the reference radon monitor mentioned
169 above.

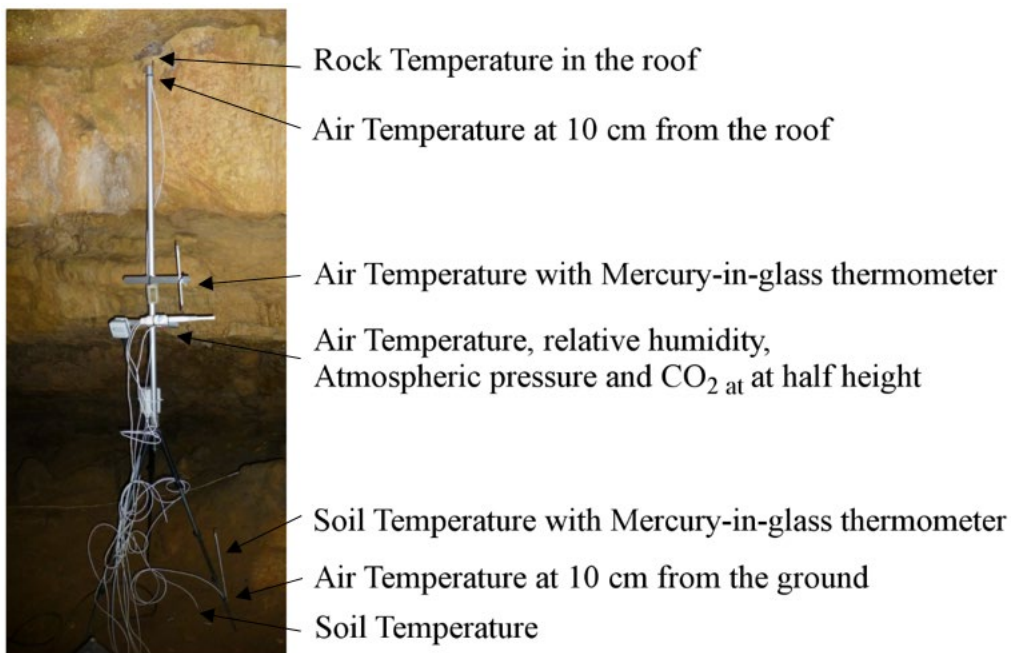
170 All radon measurements are subject to a double quality control on a continuous and periodic
171 basis. The Laboratory of Environmental Radioactivity of the University of Cantabria (LaRUC) is
172 accredited according to UNE-EN ISO/IEC 17025:2005 for integrated radon in air measurements
173 with CR-39, which implies rigorous quality control of the entire measurement process, including
174 periodic international intercomparison exercises. In this way continuous radon measurements
175 with RadonScout monitor are controlled. In addition, all available measurement systems are
176 periodically checked in the radon chamber at LaRUC, by exposing them to known concentrations
177 of radon. This chamber is a cubic container of 1 m³ volume, located in the Faculty of Medicine
178 of the University of Cantabria. The walls of the chamber consist ~~are constructed~~ of 3.25 mm
179 thick stainless steel plates welded together to ensure a tight seal. The top plate acts as a
180 removable cover for the insertion and removal of equipment and sources, and has three holes
181 that allow exposure to sets of track etch detectors without having to open the whole assembly.

182 The radon chamber is equipped for simultaneous exposure to various radon detection systems,
183 and has electrical connections to the required power sources. It also has valves to allow gas
184 exchange with the outside air, so allowing exposure to radon concentrations to be varied as
185 required. Homogeneity of the radon concentration inside the chamber is achieved using a small
186 fan, ensuring that concentration differences within the chamber are less than 3 %. The tightness
187 of the assembly is guaranteed by seals made of materials with a low diffusion coefficient for
188 radon gas; by this means, an exchange rate with the exterior of lower than 0.01 h⁻¹ is achieved.

189 **2.3 Continuous monitoring of air pressure, CO₂ concentration and air temperature**

190 For carbon dioxide and air temperature measurements, there are six stations (Fig. 2) located at
191 different points in the Cave (Exterior, Hall, Crossing, Polychromes Room, Grave Room and Well
192 Room). Each station contains several thermometers to measure air temperature at different
193 heights, CO₂ concentration, relative humidity and atmospheric pressure. Data loggers record the
194 values of each variable every 15 minutes, with daily online downloads of data. A station outside
195 the cave records the same parameters in the outdoors air.

196 The air temperature probes inside and outside are Pt100 models, with 3 x 6 mm-diameter wires,
197 40 mm long INOX AISI 316. Temperature is measured to a resolution of 0.01 °C, certified to an
198 accuracy of 0.06 °C. The probes used to determine CO₂ concentration are EE82 Series
199 instruments, are accurate to within 100 ppm and a resolution of 1 ppm. The pressure sensor is
200 a Delta OHM HD 9408, with an accuracy of 0.4 hPa at 20 °C, and a resolution of 0.01 hPa.



202 Fig. 2. Sampling station in the Hall, indicating the various sensors used for environmental
203 monitoring of the cave.

204 2.4 Air density calculation

205 As mentioned above, temperature gradients lead to variations in air density which cause
206 convective movements due to gravity. In order to study episodes of gas exchange between the
207 Polychromes Room and the exterior, the corresponding densities were evaluated over the entire
208 time series available. The calculations differ slightly for the external and internal air, taking into
209 account the high moisture content and CO₂ in the latter case. The expressions used are based
210 on the following references (Garcia-Anton et al., 2014; Buck, 1981).

211 **2.5 Estimates of exchange rates**

212 In order to assess exchange rates between the Polychromes Room and other cave chambers or
213 the exterior, the simplified model of Wilkening, used by Fernández et al. (1986), was used. This
214 mathematical model considers that the radon concentration in a chamber varies according to
215 the quantity emitted through the surface of the rocks, the quantity that disappears by
216 disintegration, and the variations produced by exchange with air masses containing different
217 concentrations from other chambers and/or the outside atmosphere.

218 The exchange rate can be calculated using the following expression, assuming that it becomes
219 practically nil when the radon concentration reaches its maximum value (Fernández et al, 1986):

$$220 \quad Q = \lambda \cdot V \cdot \frac{(C_{\max} - C)}{(C - C')} \quad (1)$$

221 where

222 Q is the exchange rate (m³/h)

223 λ is the radon disintegration constant (0.0076 h⁻¹)

224 V is the volume of the Polychromes Room (342 m³)

225 C is the radon concentration in the Polychromes Room (Bq/m³)

226 C' is the radon concentration in the chamber with which it exchanges (Bq/m³)

227 C_{\max} is the maximum annual radon concentration in Polychromes Room (Bq/m^3)

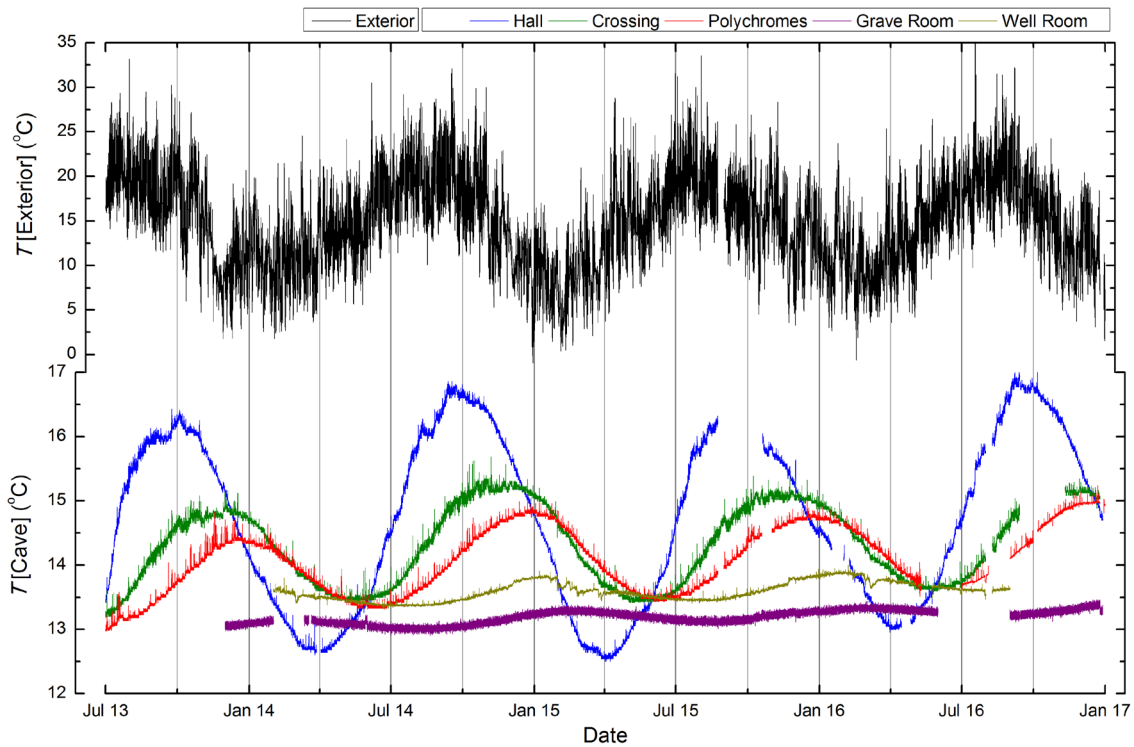
228 To estimate the exchange rate with the outside air, it can be assumed that radon concentration
229 is practically zero in the free atmosphere, therefore $C' \approx 0$.

230 **3. RESULTS AND DISCUSSION**

231 **3.1 Annual distribution of air temperature**

232 As indicated above, the air temperature field inside the Altamira Cave is fundamentally
233 determined by the annual thermal oscillations of the outside air. These oscillations are
234 transmitted into the cave through varying thicknesses of rock (Elez et al., 2013), which causes
235 the damping and lags of the thermal waves to be different in each of the interior chambers
236 (Monteith and Unsworth, 2013).

237 Fig. 3 shows air temperatures in the Exterior, Hall, Crossing and Polychromes Room between
238 2013 and 2016. The thermal wave is propagated through the rock, which attenuates its
239 amplitude and causes a lag between the outer thermal wave and the inner one. Each of the
240 temperature time series inside the cave was shifted in time to the point of maximum correlation
241 with respect to the outside temperature, and by this means information about the lag between
242 waves is obtained. The lag for the Hall is 1 month, for the Crossing, 3 months and for the
243 Polychromes Room, 4 months, according to Villar et al. (1984b, 1986a). Tab. 1 shows the
244 monthly average air temperature at half height in the Exterior, Hall and Polychromes Room.



245

246 Fig. 3. Temperature at half height inside and outside the cave for the period 2013-2016.

247 In spite of the remarkable regularity in the annual oscillation in temperature in every chamber,
 248 there are a number of degassing and recharge episodes that are related to abrupt variations in
 249 the thermal gradients between the interior and exterior parts of the cave.

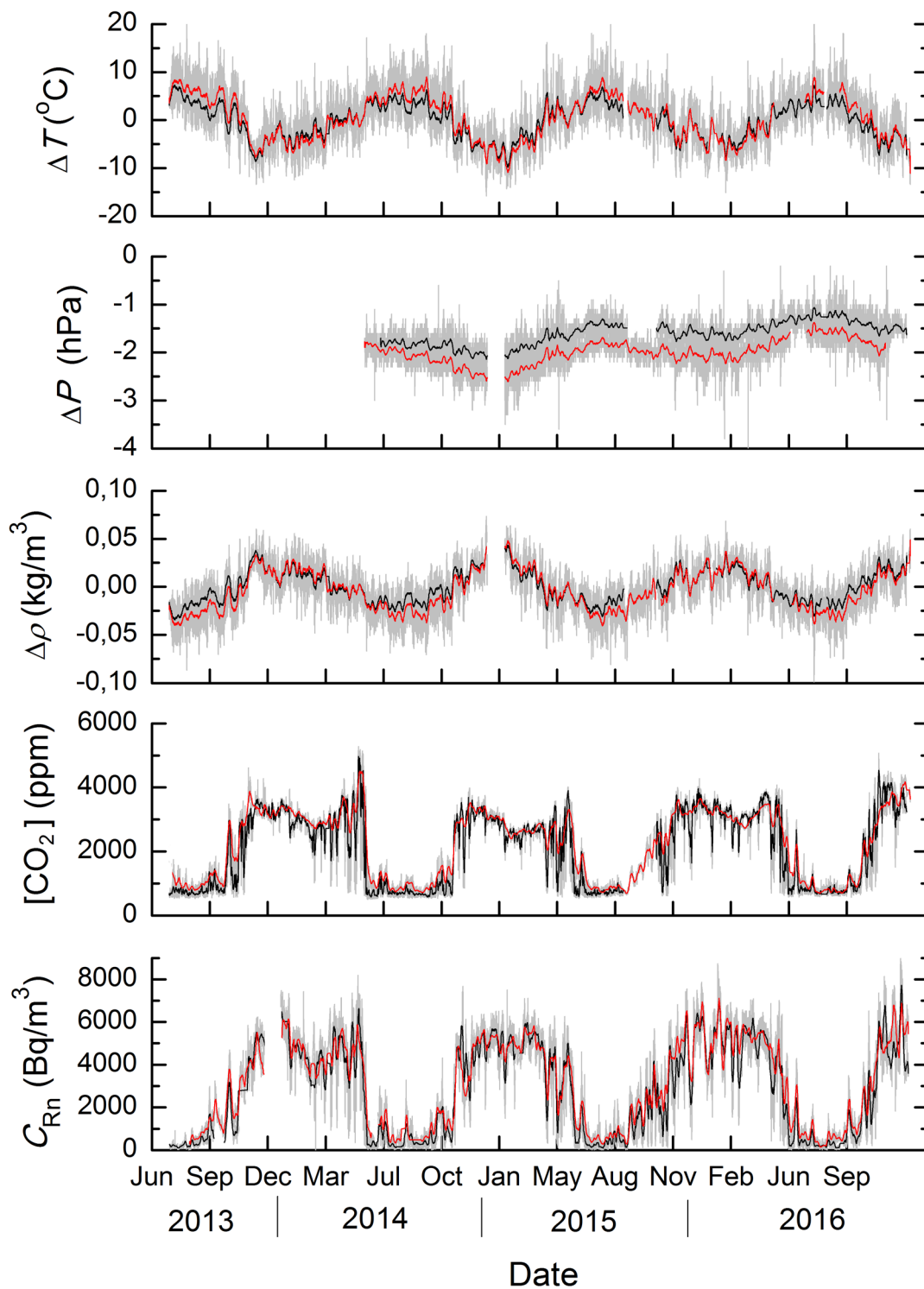
250 **3.2 Annual distribution of Rn and CO₂ concentrations**

251 As for evolution over time, there is a clear seasonal pattern in both the Hall and Polychromes
 252 Room. Concentrations in both are lowest between June and October; and highest between
 253 November and April when the exchange between the cave and the outside air is at a minimum
 254 (see Fig. 4). The monthly Rn and CO₂ concentrations in the Hall and in the Polychromes Room
 255 are shown in Tab. 1. In general, measurements in the Hall are lower than in the Polychromes
 256 Room, though this trend can be reversed during transition periods. During these transition
 257 periods, like March, oscillations in Rn concentration increase, especially near the mouth of the
 258 cave.

259 Correlations between the various chambers were calculated from the continuous data series of
260 air temperature ΔT , pressure ΔP and density $\Delta\rho$. The gradients between the Exterior and the
261 two chambers studied (Hall and Polychromes Room) are represented in Fig. 4, alongside the
262 concentrations of the tracer gases, CO_2 and Rn. Tab. 2 shows the linear correlation coefficients
263 obtained for a 95 % confidence interval and highlights how radon and carbon dioxide behaviours
264 are similar. There are small (r about -0.3) and medium (r -0.5) negative correlations between air
265 pressure and gas concentration in the Hall and Polychromes Room, respectively. On the other
266 hand, there are high negative correlations with temperature (r around -0.8), and high positive
267 correlations with air density (r around 0.8) – both higher in Polychromes Room. This indicates
268 that air temperature and density gradients dominate the behaviour of gases within the cavity.

269 Degassing in the Polychromes Room reaches its maximum expression during the summer, when
270 the average inside air temperature is much lower than outside. If exchange occurred only at the
271 cave entrance, the colder, denser air in Polychromes Room and other deeper Chambers would
272 barely reach the entrance, since these chambers lie at much lower levels than the cave mouth.
273 For these reasons, radon and carbon dioxide concentrations are at a minimum in summer, while,
274 they peak in winter when the karst matrix becomes impermeable through the combined effect
275 of accumulated moisture in the cracks and fissures, and the higher density of the outside air.
276 These observations accord with the general air dynamics described by other authors (Garcia-
277 Anton et al., 2014).

278



279

280 Fig. 4. Differences in temperature, pressure and density of the air between the Exterior and the
 281 Hall (black line) and Exterior and Polychromes Room (red line). Concentration of CO₂ and Rn in
 282 the Hall (black) and Polychromes (red). Graphs were constructed using smoothed weekly data.

283 Tab. 1. Monthly average temperature T , carbon dioxide [CO₂] and radon concentration C_{Rn} in the
 284 Exterior, Hall and Polychromes Chambers. The uncertainty of temperature is 0.06 °C, in case of
 285 CO₂ concentration is 100 ppm, and for radon concentration is found between 15 % for values
 286 around 500 Bq/m³ and 6 % about 5000 Bq/m³.

Month	Exterior	Hall			Polychromes Room		
	T (°C)	T (°C)	[CO ₂] (ppm)	C_{Rn} (Bq/m ³)	T (°C)	[CO ₂] (ppm)	C_{Rn} (Bq/m ³)
Jul-13	20.30	14.52	767	216	13.12	1134	-
Aug-13	19.22	15.73	709	335	13.26	873	636
Sep-13	18.09	15.56	915	986	13.56	1180	1443
Oct-13	16.67	15.66	1479	1322	13.90	1966	2137
Nov-13	11.03	15.51	2809	4573	14.23	3289	3949
Dec-13	9.65	14.61	3288	5034	14.38	3220	4450
Jan-14	10.34	13.79	3197	5260	14.30	3317	5146
Feb-14	9.55	13.16	2932	4553	14.10	3080	4561
Mar-14	10.63	12.73	2538	3734	13.83	2844	3849
Apr-14	13.16	12.76	2954	4781	13.57	3092	4933
May-14	13.45	13.18	3237	4692	13.40	3552	4554
Jun-14	17.43	13.97	982	656	13.36	1568	1795
Jul-14	18.83	15.07	801	556	13.47	974	901
Aug-14	19.10	16.05	731	550	13.70	912	855
Sep-14	19.83	16.61	672	387	14.03	828	701
Oct-14	17.83	16.53	910	917	14.38	1289	1452
Nov-14	13.26	16.06	2650	3759	14.64	2755	3217
Dec-14	9.48	15.22	3177	4500	14.79	3335	4878
Jan-15	8.39	14.31	2939	5112	14.76	3043	5051
Feb-15	7.13	13.24	2455	4647	14.50	2566	4844

Mar-15	9.83	12.68	2649	5507	14.11	2669	5357
Apr-15	13.88	12.67	2495	4017	13.77	2661	4060
May-15	14.71	13.20	2286	3025	13.54	2624	3184
Jun-15	17.49	13.95	858	629	13.48	1354	1185
Jul-15	19.91	15.31	713	263	13.57	812	497
Aug-15	19.60	16.03	778	499	13.76	850	695
Sep-15	16.41	-	-	1310	14.11	1269	1668
Oct-15	15.37	15.80	2096	2293	14.43	2189	2584
Nov-15	13.51	15.54	2466	3115	14.62	2896	3970
Dec-15	13.05	14.80	3185	4685	14.73	3263	5087
Jan-16	10.73	14.42	3330	5020	14.69	3377	5135
Feb-16	9.37	13.82	3182	5373	14.53	3179	5554
Mar-16	9.50	13.26	2937	4944	14.24	2893	5407
Apr-16	11.55	13.05	3436	5282	13.91	3289	5252
May-16	14.78	13.45	2527	3376	13.73	2937	3905
Jun-16	17.09	14.23	1115	795	13.69	1592	1566
Jul-16	19.32	15.29	804	357	13.75	887	618
Aug-16	19.96	16.30	764	239	13.84	785	519
Sep-16	18.58	16.78	883	827	14.25	942	1081
Oct-16	14.99	16.55	1870	1928	14.67	1961	2349
Nov-16	11.02	15.96	3702	4828	14.89	3354	4913
Dec-16	11.42	15.11	3452	5049	14.97	3802	5793

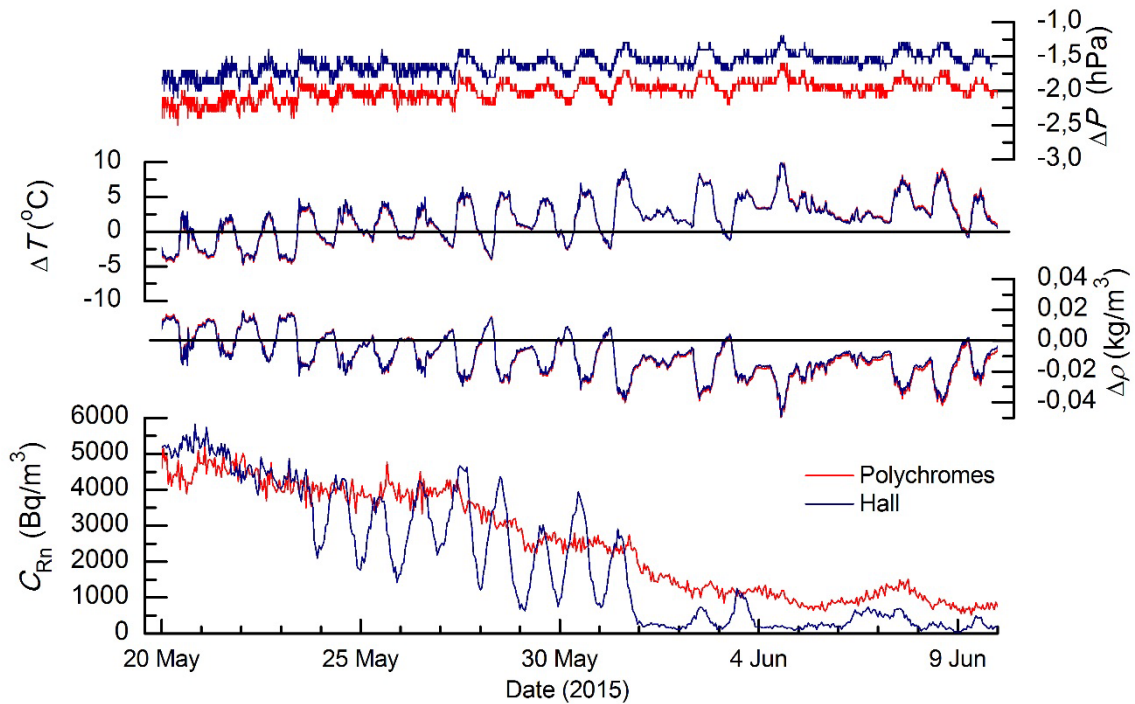
287

288 Tab. 2. Linear correlation coefficient, r , between the difference in air pressure, density and
289 temperature in the Exterior and inside Altamira Cave (Hall and Polychromes Room) with tracer
290 gases, CO₂ and Rn, obtained for a 95 percent confidence interval.

	[CO ₂] (ppm)	C _{Rn} (Bq/m ³)
ΔP (Ext.-Hall)	-0.28 (-0.34 to -0.21)	-0.34 (-0.40 to -0.27)
$\Delta \rho$ (Ext.-Hall)	0.77 (0.75 to 0.80)	0.75 (0.72 to 0.77)
ΔT (Ext.-Hall)	-0.79 (-0.80 to -0.76)	-0.76 (-0.78 to -0.73)
ΔP (Ext.-Poly.)	-0.53 (-0.57 to -0.48)	-0.51 (-0.56 to -0.46)
$\Delta \rho$ (Ext.-Poly.)	0.80 (0.78 to 0.82)	0.82 (0.78 to 0.84)
ΔT (Ext.-Poly.)	-0.81 (-0.83 to -0.79)	-0.82 (-0.84 to -0.80)

291

292 Having demonstrated the capacity of continuous radon monitoring to describe the movement
293 of air masses inside the cave and air exchanges with the outside air over annual periods, we
294 analysed the degassing and recharge events evident over shorter periods. There are two periods
295 in the year when fluctuations in Rn and CO₂ concentrations are significant, namely the season
296 changes from spring to summer and from summer to autumn. During these periods, abrupt
297 variations in trace gas concentrations can be observed over a single day or even just a few hours,
298 which may be related to the highly variable diurnal alternations in external temperatures. We
299 present an analysis of the period May 20 to June 9, 2015, where varieties of the above-
300 mentioned short-period fluctuations were observed.



301

302 Fig. 5. Air pressure, temperature and density differences between the external atmosphere and
 303 Polychromes Room (red line) and Hall (blue line) for the period 20 May to 10 June, 2015. The
 304 radon variation in each chamber is also shown.

305 Fig. 5 shows the difference in air pressure, temperature and density between the outside
 306 atmosphere, the Polychromes Room and the Hall for the period 20 May to 10 June, 2015. Radon
 307 concentrations in the Hall and Polychromes decreased from 5000 Bq/m³ to below 1000 Bq/m³.
 308 At this time of year the temperature of these two chambers is practically the same – as can be
 309 seen on a large scale in Fig. 3, or in detail in Fig. 5. There is a difference in their average
 310 temperatures over this period of less than 0.1 °C.

311 Chamber degassing occurs when the air density gradient is negative, *i.e.*, the density of the
 312 outside air is lower than the density of the indoor air ($\rho_{\text{ext}} < \rho_{\text{cave}}$). The denser air inside the cave
 313 tends to descend to lower levels through the pores and cracks of the karst, so favouring the
 314 observed decrease in the concentration of Rn. The greater degree of connection between the
 315 Hall and the Exterior means that degassing and recharge of this chamber is more pronounced
 316 than for the Polychromes Room. A strong correlation is found between the difference between

317 Exterior-Hall densities and the concentration of Rn. The results of the correlation analysis are
 318 shown in Tab. 3.

319 Tab. 3. Linear correlation coefficient r between the difference in air pressure, density and
 320 temperature in the Exterior and in the Cave (Hall or Polychromes Room) with Rn concentration
 321 obtained for a 95 percent confidence interval for the period 20 May to 10 June 2015 (event
 322 shown in Fig. 5).

	C_{Rn} [Hall] (Bq/m ³)	C_{Rn} [Polychromes] (Bq/m ³)
ΔP (Ext.- Chamber)	-0.08(-0.17 to -0.01)	-0.11 (-0.19 to -0.01)
$\Delta\rho$ (Ext.- Chamber)	0.48 (0.40 to 0.54)	0.59 (0.53 to 0.64)
ΔT (Ext.- Chamber)	-0.48 (-0.54 to -0.41)	-0.59 (-0.53 to -0.64)

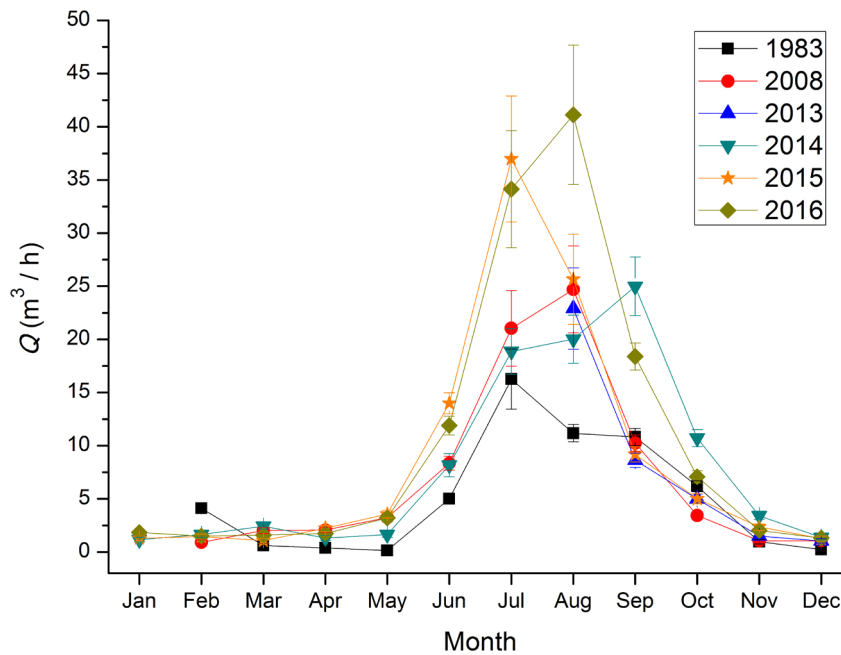
323

324 **3.3 Degree of connection between the chambers and with the exterior**

325 The first estimates of the rates of gaseous exchange between the Polychromes Room and the
 326 rest of the Cave were made in the 1980s (Fernández et al., 1986). The estimates were made
 327 based on the hypothesis that the most intense convective air exchange was with the Hall,
 328 occurring mainly by circulation through The Crossing. It was assumed that the restricted
 329 connection of the various chambers of the cave with the exterior meant that the predominant
 330 mechanism for mass air movement was due to air temperature gradients established inside in
 331 the cave. A second door was installed in 2008 at the point where the Hall joins The Crossing. This
 332 radically modified the route for air exchange between the Hall and the Polychromes Room; but
 333 it also highlighted the importance of the fissures and cracks in the karst as an alternative route
 334 for air exchange with the outside atmosphere (Sánchez-Moral et al., 2009). The thermal
 335 gradients between the air in the Polychromes Room and the other chambers deeper in the cave
 336 are negative throughout the year (Fig. 3). Given the other chambers are at a lower level than the
 337 Polychromes Room, air exchange between the various chambers seemed unlikely. For these

338 reasons, estimates of the rates of gaseous exchange in the Polychromes Room are made
 339 assuming that these exchanges occurred preferentially with the exterior through the voids of
 340 the karst on the basis of historic and contemporary data on radon concentrations.

341 The exchange rate between the Polychromes Room and the outside was estimated from Eq. (1)
 342 and the monthly mean values of radon concentration are summarised in Tab. 1. The maximum
 343 annual radon concentration C_{max} is shown in Tab. 4, the volume of Polychromes Room is 342 m^3
 344 and the radon concentration from the outside C' was assumed to be zero. The results of the
 345 monthly exchange rate for 1983, 2008 and for the period 2013-2016 are given in Tab. 4, while
 346 they are displayed graphically in Fig. 6.



347

348 Fig. 6. Monthly variations in the ventilation rate Q (m^3/h) between the Polychromes Room and
 349 the outside in 1983 (Fernández et al., 1986), 2008 (Sánchez-Moral et al., 2009) and the period
 350 2013-2016.

351 The extraordinary increase in the rate of ventilation during the summer months might be
 352 explained by the significantly higher average temperature over this period. The greater
 353 difference in air densities in recent years, might have provoked greater degassing and enhanced

354 connection of the chamber with the outside air. This explanation will need to be validated by
 355 collecting further data on annual cycles.

356 Tab. 4. Monthly ventilation rate Q (m^3/h) between the Polychromes Room and the outside in
 357 1983 (Fernández et al., 1986), 2008 (Sánchez-Moral et al., 2009) and the period 2013-2016.

358 Maximum annual radon concentration C_{max} (Bq/m^3) is also given.

Month	1983	2008	2013	2014	2015	2016
January	-	-	-	1.16 ± 0.23	1.29 ± 0.23	1.82 ± 0.27
February	4.10 ± 0.40	0.91 ± 0.21	-	1.64 ± 0.25	1.46 ± 0.24	1.49 ± 0.25
March	0.60 ± 0.19	2.03 ± 0.28	-	2.42 ± 0.30	1.07 ± 0.22	1.60 ± 0.25
April	0.38 ± 0.18	2.06 ± 0.28	-	1.32 ± 0.24	2.24 ± 0.29	1.72 ± 0.26
May	0.15 ± 0.17	3.22 ± 0.35	-	1.65 ± 0.25	3.57 ± 0.37	3.21 ± 0.35
June	5.00 ± 0.46	8.34 ± 0.66	-	8.1 ± 1.1	14.0 ± 1.0	11.90 ± 0.87
July	16.3 ± 2.8	21.0 ± 3.6	-	18.9 ± 2.2	37.0 ± 5.9	34.1 ± 5.5
August	11.17 ± 0.83	24.7 ± 4.1	22.9 ± 3.8	20.0 ± 2.3	25.7 ± 4.2	41.1 ± 6.6
September	10.81 ± 0.81	10.25 ± 0.77	8.64 ± 0.68	25.0 ± 2.8	9.18 ± 0.71	18.4 ± 1.3
October	6.18 ± 0.53	3.43 ± 0.36	4.99 ± 0.46	10.71 ± 0.80	5.01 ± 0.46	7.07 ± 0.58
November	0.96 ± 0.21	1.05 ± 0.22	1.51 ± 0.25	3.41 ± 0.36	2.35 ± 0.30	2.02 ± 0.28
December	0.23 ± 0.17	1.05 ± 0.22	1.04 ± 0.22	1.36 ± 0.24	1.26 ± 0.23	1.32 ± 0.24
C_{max} (Bq/m^3)	7250 ± 440	7250 ± 430	6240 ± 370	7440 ± 450	7560 ± 450	8730 ± 520

359

360 4. CONCLUSIONS

361 The concentrations of radon gas inside Altamira Cave can be used as an indicator of air
 362 movements both within the cave and in exchanges with the outside atmosphere. Its role as a
 363 tracer has been demonstrated to be valid both to reflect the seasonal cycles of degassing and
 364 recharge, and to analyse shorter (daily) period fluctuations.

365 Although air pressure and density are related magnitudes, air density gradients prove to be more
366 sensitive indicators of convective motion than air pressure differences. Although the latter
367 explain long-term aerodynamic changes with a relatively good precision, they are limited when
368 it comes to predicting short-term exchanges.

369 We have verified that the connection of the Polychromes Room with the rest of the cave was
370 drastically reduced by the installation of the second closure in 2008. Except for point exchanges
371 with The Crossing generated by a negative temperature gradient in that direction, the
372 atmosphere of the Polychromes Room remains stable, or else it exchanges matter with the
373 exterior through the karst interface.

374 The annual distribution of temperature in the Hall and Polychromes Room has been updated;
375 we observed a warming trend that could be related to a rising trend in exterior temperature.
376 This warming could explain the increase observed in the ventilation rate between the
377 Polychromes Room and the outer atmosphere. This needs to be corroborated with further
378 specific analyses. Likewise, knowledge of the dynamics of the air inside the cave has been
379 updated using radon gas as a tracer.

380 The distribution of the concentrations of radon and CO₂ present significant parallels. However,
381 there are many situations of divergence of this trend, attributable to the different chemical
382 behaviours and origins of both gases. The greater diversity and complexity of mechanisms of
383 generation and disappearance of the carbon dioxide in the air, makes it more complicated to
384 implement mathematical models that focus on the to evaluate quantitative exchanges of air
385 masses between different rooms. This observation leads us to recommend radon gas
386 concentration as a tracer, mainly due to the simpler mechanisms involved in the rises and falls
387 in its concentration.

388 **5. ACKNOWLEDGEMENTS**

389 The authors are grateful to the Altamira Cave Research Centre and Museum staff for their
390 helpful support during the sampling surveys in the cave. This research was funded by the Project
391 “Estudios analíticos para una propuesta de accesibilidad pública de la Cueva de Altamira” funded
392 by the Ministry of Education, Culture and Sport of Spain (MECD). We also acknowledge the
393 essential collaboration of the Spanish Meteorological Agency (AEMET).

394 6. REFERENCES

395

396 Batiot-Guilhe, C., Seidel, J. L., Jourde, H., Hébrard, O., & Bailly-Comte, V. (2007). Seasonal
397 variations of CO₂ and ²²²Rn in a Mediterranean sinkhole-spring (Causse d’Aumelas, SE
398 France). *International Journal of Speleology*, 36(1), 5.

399 Buck, A. L. (1981). New equations for computing vapor pressure and enhancement
400 factor. *Journal of applied meteorology*, 20(12), 1527-1532.

401 Cuezva, S., Fernández-Cortes, A., Benavente, D., Serrano-Ortiz, P., Kowalski, A. S., & Sánchez-
402 Moral, S. (2011). Short-term CO₂ (g) exchange between a shallow karstic cavity and the external
403 atmosphere during summer: role of the surface soil layer. *Atmospheric Environment*, 45(7),
404 1418-1427. [10.1016/j.atmosenv.2010.12.023](https://doi.org/10.1016/j.atmosenv.2010.12.023)

405 Déchelette, J. (1908). *Manuel d'archéologie préhistorique celtique et gallo-romaine. Archéologie*
406 *préhistorique*. Paris (France) A Picard et fils.

407 Elez, J., Cuezva, S., Fernández-Cortes, A., Garcia-Antón, E., Benavente, D., Cañaveras, J. C., &
408 Sánchez-Moral, S. (2013). A GIS-based methodology to quantitatively define an Adjacent
409 Protected Area in a shallow karst cavity: The case of Altamira cave. *Journal of environmental*
410 *management*, 118, 122-134. [10.1016/j.jenvman.2013.01.020](https://doi.org/10.1016/j.jenvman.2013.01.020)

411 Fernández, P. L., Quindós, L. S., Soto, J., & Villar, E. (1984). Radiation exposure levels in Altamira
412 Cave. *Health physics*, 46(2), 445-448.

413 Fernández, P. L., Gutierrez, I., Quindós, L. S., Soto, J., & Villar, E. (1986). Natural ventilation of
414 the paintings room in the Altamira cave. *Nature*, 321(6070), 586-588. [10.1038/321586a0](https://doi.org/10.1038/321586a0)

415 Frisia, S., Fairchild, I. J., Fohlmeister, J., Miorandi, R., Spötl, C., & Borsato, A. (2011). Carbon mass-
416 balance modelling and carbon isotope exchange processes in dynamic caves. *Geochimica et*
417 *Cosmochimica Acta*, 75(2), 380-400. [10.1016/j.gca.2010.10.021](https://doi.org/10.1016/j.gca.2010.10.021)

418 Garcia-Anton, E., Cuezva, S., Fernández-Cortes, A., Benavente, D., Sánchez-Moral, S. (2014).
419 Main drivers of diffusive and advective processes of CO₂-gas exchange between a shallow
420 vadose zone and the atmosphere. *International Journal of Greenhouse Gas Control*, 21, 113-129.
421 [10.1016/j.ijggc.2013.12.006](https://doi.org/10.1016/j.ijggc.2013.12.006)

422 George, A. C. (1996). State-of-the-Art Instruments for Measuring Radon/thoron and Their
423 Progeny in Dwellings-A Review. *Health physics*, 70(4), 451-463. PMID: 8617584

424 Kowalczk, A. J., & Froelich, P. N. (2010). Cave air ventilation and CO₂ outgassing by radon-222
425 modeling: how fast do caves breathe?. *Earth and Planetary Science Letters*, 289(1), 209-219.
426 [10.1016/j.epsl.2009.11.010](https://doi.org/10.1016/j.epsl.2009.11.010)

427 Lario, J., Sánchez-Moral, S., Cañaveras, J. C., Cuezva, S., & Soler, V. (2005). Radon continuous
428 monitoring in Altamira Cave (northern Spain) to assess user's annual effective dose. *Journal of*
429 *Environmental Radioactivity*, 80(2), 161-174. [10.1016/j.jenvrad.2004.06.007](https://doi.org/10.1016/j.jenvrad.2004.06.007)

430 Lasheras, J.A.; De Las Heras, C.; Prada, A. (2014): *Altamira and its future*. En: SAIZ-JIMÉNEZ, C.
431 (Ed.): The conservation of subterranean cultural heritage, Londres. CRC Press, p.145-164.

432 Monteith, J., & Unsworth, M. (2013). Principles of environmental physics: plants, animals, and
433 the atmosphere. Academic Press. 4th Ed.

434 Moreno, V., Font, Ll., Baixeras, C., Garcia-Orellana, J., Bach, J., Grossi, C., Vargas, A. (2015)
435 Effectiveness Analysis of Filters Used with Radon Detectors under Extreme Environmental

436 Conditions for Long-term Exposures. *Physics Procedia*, 80, 113-116.
437 [10.1016/j.phpro.2015.11.067](https://doi.org/10.1016/j.phpro.2015.11.067)

438 Nazaroff, W. W., & Nero Jr, A. V. (1988). *Radon and its decay products in indoor air*. New York
439 NY, Wiley and Sons

440 Pfendler, S., Karimi, B., Maron, P. A., Ciadamidaro, L., Valot, B., Boust, F., ... & Aleya, L. (2018).
441 Biofilm biodiversity in French and Swiss show caves using the metabarcoding approach: First
442 data. *Science of The Total Environment*, 615, 1207-1217. [10.1016/j.scitotenv.2017.10.054](https://doi.org/10.1016/j.scitotenv.2017.10.054)

443 Quindós, L. S., Fernández, P. L., & Soto, J. (1991). National survey on indoor radon in
444 Spain. *Environment international*, 17(5), 449-453. [10.1016/0160-4120\(91\)90278-X](https://doi.org/10.1016/0160-4120(91)90278-X)

445 Sainz, C., Rábago, D., Fuente, I., Celaya, S., & Quindós, L. S. (2016). Description of the behavior
446 of an aquifer by using continuous radon monitoring in a thermal spa. *Science of The Total
447 Environment*, 543, 460-466. [10.1016/j.scitotenv.2015.11.052](https://doi.org/10.1016/j.scitotenv.2015.11.052)

448 Sánchez-Moral, S., Soler, V., Cañaveras, J. C., Sanz-Rubio, E., Van Grieken, R., & Gysels, K. (1999).
449 Inorganic deterioration affecting the Altamira Cave, N Spain: quantitative approach to wall-
450 corrosion (solutional etching) processes induced by visitors. *Science of the Total
451 Environment*, 243, 67-84. [10.1016/S0048-9697\(99\)00348-4](https://doi.org/10.1016/S0048-9697(99)00348-4)

452 Sánchez-Moral, S., Cuezva, S., Fernández-Cortés, A., Janices, I., Benavente, D., Cañaveras, J. C.,
453 ... & Portillo, M. C. (2009). Estudio integral del estado de conservación de la Cueva de Altamira
454 y sus representaciones artísticas paleolíticas. Perspectivas futuras de conservación. *Report for
455 the Dirección General de Bellas Artes y Bienes Culturales, Ministerio de Educación, Cultura y
456 Deporte*.

457 Sánchez-Moral, S., Cuezva, S., Fernández-Cortés, A., Benavente, D., & Cañaveras, J. C. (2010).
458 Effect of ventilation on karst system equilibrium (Altamira Cave, N Spain): an appraisal of karst
459 contribution to the global carbon cycle balance. *Advances in Research in Karst Media*, 469-474.

460 Sánchez-Moral, S., Portillo, M. C., Janices, I., Cuezva, S., Fernández-Cortés, A., Cañaveras, J. C., &
461 Gonzalez, J. M. (2012). The role of microorganisms in the formation of calcitic moonmilk deposits
462 and speleothems in Altamira Cave. *Geomorphology*, 139, 285-292.
463 [10.1016/j.geomorph.2011.10.030](https://doi.org/10.1016/j.geomorph.2011.10.030)

464 Soler, V.; Sánchez, S.; Cañaveras, J. C.; Sanz, E.; Lasheras, J. A.; Lario, J. (1999).
465 Microenvironmental monitoring system at Altamira cave (northern Spain). 2nd International
466 Congress on Science and Technology for the Safeguard of Cultural Heritage in the Mediterranean
467 Basin (A. Guarino, A. Ferrari eds.), pp. 304. Paris.

468 Somavilla, J. F., Khayyat, N., & Arroyo, V. (1978). A comparative study of the microorganisms
469 present in the Altamira and La Pasiega caves. *International biodeterioration bulletin*, 14(4), 103-
470 109.

471 Villar, E., Fernández, P. L., Quindós, L. S., Solana, J. R. & Soto, J. (1983). Temperature of rock art
472 surfaces in Altamira cave (Spain). *Cave Science*, 10 (3), 165-170.

473 Villar, E., Fernández, P. L., Quindós, L. S., Solana, J. R., & Soto, J. (1984a). Air temperatures and
474 air interchanges at Altamira Cave (Spain). *Cave Science*, 11(2), 92-98.

475 Villar, E., Bonet, A., Díaz-Caneja, B., Fernández, P. L., Gutierrez, I., Quindós, L. S., ... & Soto, J.
476 (1984b). Ambient temperature variations in the hall of paintings of Altamira cave due to the
477 presence of visitors. *Cave Science*, 11(2), 99-104.

478 Villar, E., Fernández, P. L., Quindós, L. S. & Soto, J. (1985). Natural temporal evolution of the CO₂
479 content in the air of the "Painting Chamber" at Altamira cave. *National Speleological Society*
480 *Bulletin*, 47 (1), pp. 12-16.

481 Villar, E. (1986a). Propagación de la onda térmica anual a través de discontinuidades de aire
482 subterráneas. *Anales de Física*, serie B, 82, 132-142.

483 Villar, E., Fernández, P. L., Gutierrez, I., Quindós, L. S., & Soto, J. (1986b). Influence of visitors on
484 carbon concentrations in Altamira Cave. *Cave Science*, 13(1), 21-23.